A novel energy efficient controllable stiffness joint

David Ball *Member, IEEE*, Patrick Ross, James Wall, Ricky Chow

***Abstract* — Achieving energy efficient legged locomotion is an important goal for the future of robot mobility. This paper presents a novel joint for legged locomotion that is energy efficient for two reasons. The first reason is the configuration of the elastic elements and actuator which we show analytically has lower energy losses than the typical arrangement. The second is that the joint stiffness, and hence stance duration, is controllable without requiring any energy from the actuator. Further, the joint stiffness can be changed significantly during the flight phase, from zero to highly rigid. Results obtained from a prototype hopper, demonstrate that the joint allows continuous and peak hopping via torque control. The results also demonstrate that the hopping frequency can be varied between 2.2Hz and 4.6Hz with associated stance duration of between 0.35 and 0.15 seconds.**

I. INTRODUCTION

Legged animals run efficiently due to elastic elements providing a cyclic conversion between kinetic and potential energy. The Spring-Loaded Inverted Pendulum (SLIP) model [1] is a widely used model of legged locomotion, approximating the leg as an ideal spring supporting a point mass body. Mimicking SLIP motion and its inherent energy efficiency is important for the future of robot mobility. To achieve this means designing leg joints that combine elastic elements and actuators to perform the mechanical work of SLIP motion, while minimising actuator power loss.

There are three contributions in this paper. The first is an analytical derivation which shows that the configuration of our joint is more energy efficient than the typical configuration as the actuator will have lower losses while still doing the same mechanical work for SLIP motion. The second is the conceptual design of the joint that shows how to overcome caveats in the configuration to allow energy efficient control of critical gait parameters. The third is the implementation of the joint into a hopping robot and the corresponding results that demonstrate the joint's performance is due to its configuration.

The joint is designed so that the SLIP motion trajectory can be controlled by changing joint stiffness in a single flight phase. Changing joint stiffness will change hopping frequency and stance duration which are critical for gait control. Joint stiffness could be changed in response to varying ground hardness, a change in desired gait trajectory, and to respond to disturbance. This gait control behaviour is similar to how human runners change leg stiffness during flight phase when transitioning between surfaces of differing hardness [2]. Importantly, in our proposed design, energy is not required from the actuator to change or maintain stiffness. The joint stiffness can be varied from zero, giving complete torque control to the actuator, to highly rigid which completely supports the body mass without actuator energy. This ability to support the body mass without actuator energy is only possible due to the configuration of the joint. The energy efficient controllable stiffness joint (EECSJ) is shown in Figure 1. The joint uses a new linear actuator that has a high power to mass ratio and is coupled between the links without requiring a gearbox.

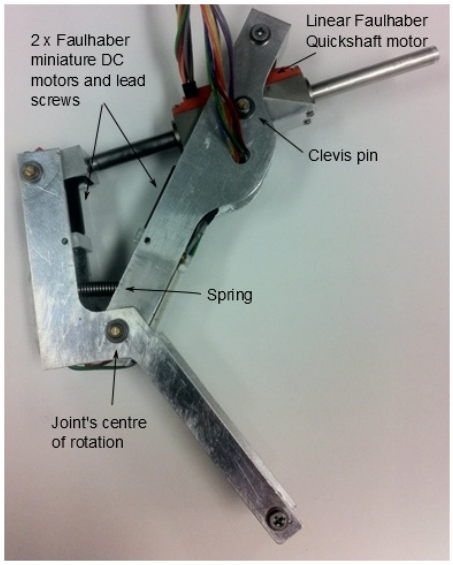

Figure 1: The energy efficient controllable stiffness joint with the stiffness mechanism set at approximately 60% of the distance along the lead screws.

II. BACKGROUND

The majority of elastic actuator mechanisms are based on the series elastic actuator configuration, SEA [3]. The SEA has the advantage of high bandwidth mechanical compliance and force control. To increase suitability for different situations, a number of mechanisms extend the SEA allowing what is termed variable, adjustable or controllable stiffness.

An Actuator with Mechanically Adjustable Series Compliance (AMASC) [4] prototype uses cable driven differential and series springs and pulleys to store energy and allow adjustment of joint stiffness with low friction and zero backlash. An Actuator with Adjustable Stiffness, AwAS [5] and AwAS-II [6] allows a wide range of joint stiffness to be regulated with minimal energy consumption because the position of the series spring is controlled. The Mechanically Adjustable Compliance and Controllable Equilibrium Position Actuator MACCEPA 2.0 [7] allows the

D. Ball and P. Ross are with the School of Electrical Engineering and Computer Science at the Queensland University of Technology, QLD, Australia (e-mail: david.ball@qut.edu.au).

J. Wall and R. Chow are with the School of Information Technology and Electrical Engineering at the University of Queensland, QLD, Australia.

stiffness-angle curve to be set by choosing an appropriate shape for a profile disk. The VS-Joint [8] is a variable stiffness joint where a small motor controls the vertical position of the spring slider to pre compress the springs.

III. Comparison of Elastic Configurations

The configurations reviewed in the previous section are all SEAs. However, as we demonstrate analytically in this section, the SEA is less energy efficient than the PEA as a design for SLIP motion. In order to focus this comparison on the core principle of energy efficiency, a complete leg and mass model has been reduced into a minimal set of fundamental components as shown in Figure 2.

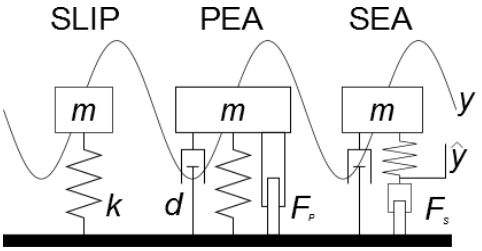

Figure 2: The spring loaded inverted pendulum (SLIP), parallel elastic actuator (PEA), and series elastic actuator (SEA) configurations. The diagram includes the mass, spring, damper, and actuator force.

This section compares the PEA and SEA configurations in regard to the work performed by the actuator and the energy lost in the actuator. The most energy efficient configuration is the one where less energy is consumed for the same amount of work. The control law used as the basis for this comparison is as required to emulate SLIP motion, assuming no disturbances. For brevity of derivation, the 'toe' is fixed to the ground and hence work and energy are calculated over one entire SLIP cycle. Unforced SLIP motion is given by

$$m\ddot{y} + ky = -mg \tag{1}$$

where k is the spring constant, m is the body mass and g is gravity. In the Laplace domain, $Y(s)$, this is

$$Y(s) = \frac{s^2y(0)+s\dot{y}(0)-g}{s(s^2+\frac{k}{m})} \tag{2}$$

where $y(0)$ and $\dot{y}(0)$ are the initial position and velocity of the mass and the solution for the position at time t is

$$y(t) = \left(y(0) + \frac{mg}{k}\right)\cos(\omega t) + \frac{\dot{y}(0)}{\omega}\sin(\omega t) - \frac{mg}{k} \tag{3}$$

where ω is the frequency of oscillation and is given by

$$\omega = \sqrt{\frac{k}{m}} \tag{4}$$

Equation 3 can also be written in the form

$$y(t) = A\sin(\omega t + \theta) - \frac{mg}{k} \tag{5}$$

$$y(\hat{t}) = A\sin(\omega \hat{t}) - \frac{mg}{k} \tag{6}$$

$$\dot{y}(\hat{t}) = A\omega\cos(\omega \hat{t}) \tag{7}$$

where t has been replaced with $\hat{t}$ for simplification as

$$\hat{t} = t - \frac{\theta}{\omega} \tag{8}$$

and

$$A^2 = \left(y(0) + \frac{mg}{k}\right)^2 + \left(\frac{\dot{y}(0)}{\omega}\right)^2 \tag{9}$$

For the PEA configuration, the equation of motion is

$$m\ddot{y} + d\dot{y} + ky = F_P - mg \tag{10}$$

where d is the damping of the system. Assuming no disturbance the actuator must supply F_P as given by

$$F_P = d\dot{y} = dAw\cos(\omega \hat{t}) \tag{11}$$

where $\dot{y}$ comes from Equation 7. The work performed by the actuator, W_P over a complete cycle is given by

$$W_P = \int_0^{\frac{2\pi}{\omega}} F_P\dot{y}\,\partial\hat{t} \tag{12}$$

$$W_P = dA^2\omega\pi \tag{13}$$

For the SEA, because of the extra motion between the actuator and spring, there are two equations of motion. Assuming the link between the spring and actuator is massless, the force supplied by the actuator, F_S, must equal the spring force

$$m\ddot{y} + d\dot{y} + ky = k\hat{y} - mg \tag{14}$$

$$F_S = -k(y - \hat{y}) \tag{15}$$

where $\hat{y}$ is the position where the actuator is connected to the spring. The actuator must supply F_S, given by

$$F_S = d\dot{y} - ky = dA\omega\cos(\omega \hat{t}) - kA\sin(\omega \hat{t}) + mg \tag{16}$$

Over a distance of

$$\hat{y} = \frac{d\dot{y}}{k} = \frac{dA}{k}\omega\,cos\,(\omega \hat{t}) \tag{17}$$

the work performed by the actuator, W_S, over a complete cycle is given by

$$W_S = \int_0^{\frac{2\pi}{\omega}} F_S\,\dot{\hat{y}}\,\partial\hat{t} \tag{18}$$

$$W_S = dA^2\omega\pi \tag{19}$$

Therefore, since W_S is equal to W_P, the work performed by the SEA and PEA configuration is equal.

In an electromechanical system the power losses are predominantly in the actuator and are proportional to the current squared where current is proportional to force, solving over a complete cycle

$$E \propto \int_0^{\frac{2\pi}{\omega}} I^2\partial\hat{t} \propto \int_0^{\frac{2\pi}{\omega}} F^2\partial\hat{t} \tag{20}$$

For the PEA, the actuator must supply F_P therefore, the energy losses in the PEA,E_P, after solving the integral are given by

$$E_P = A^2d^2\omega\pi \tag{21}$$

Similarly for the SEA, the actuator must supply, F_S therefore the energy losses in the SEA, E_S, are given by

$$E_S = A^2d^2\omega\pi + \frac{\pi}{\omega}(A^2k^2 + 2m^2g^2) \tag{22}$$

Comparing, the SEA configuration losses, E_S, has an extra positive term over the PEA configuration losses, E_P, hence the PEA is more energy efficient.

As mentioned previously, this derivation can be extended for the more precise case of a hopping leg where the actuator supplies energy only during the stance phase. The result, that the PEA is more energy efficient, remains the same.

IV. EECSJ Design Concept

The previous section demonstrated that the PEA configuration is more energy efficient for SLIP motion, however there are two issues that must be addressed. This section describes how the EECSJ addresses these two issues.

The first issue is that energy efficient legged locomotion relies on changing joint stiffness to maintain optimal body mass trajectory for gait control and variable ground hardness. Studies demonstrate that running humans change their effective leg stiffness by a large amount during a single flight phase to compensate for changing ground hardness [2]. For a fixed stiffness PEA, using the typically required strong springs, the actuator will have to work hard to oscillate at frequencies other than the spring's natural frequency. Therefore, to be energy efficient across ground of varying hardness while also controlling gait trajectory, the joint requires controllable stiffness.

The joint addresses this first issue with a parallel controllable stiffness configuration which allows the joint stiffness to be changed from highly rigid, where the spring supports the body mass, to zero stiffness. Note that this inherent ability to make the joint highly rigid without any actuator energy is another advantage of the parallel arrangement, as in the series arrangement the actuator will freely move when no power is supplied. The implementation section shows that the stiffness mechanism is also self locking against change, which means that unlike other designs no energy needs to be continuously supplied to maintain a desired stiffness. It is expected that the energy consumed to change stiffness to handle variations in surface hardness and control gait will be much smaller than the energy consumed to maintain hopping.

The second issue is that force control is required in order to realise the controller outlined previously for SLIP motion. This is due to position control mismatches between the spring and real actuators. Force control is challenging for actuators with large gear ratios due to their high reflected inertia, hence our design does not use a gearbox. The joint addresses this second issue by using a new linear actuator with direct coupling that does not require a gearbox.

From this point on the paper switches from a prismatic to a revolute joint configuration, therefore switching position with angle and force with torque. These are equivalent in regard to energy and work. The actuator and elastic mechanisms combine to generate a torque τ_j about the joint's centre of rotation given by

$$\tau_j = \tau_s + \tau_d \tag{23}$$

where τ_s is the torque contributed by the controllable stiffness mechanism and τ_d is the torque generated by the actuator.

A. Controllable stiffness mechanism

Inspired by how humans adjust their muscle stiffness between strides when running, this joint is designed so that stiffness can be changed during the flight phase. The concept behind the controllable stiffness mechanism is that the effective joint stiffness is dependent on the rate of change of the spring extension due to a change in moment arm distance from the joint's centre of rotation. This controllable stiffness concept is similar to that found in the AwAS I and II designs however here we focus on a parallel configuration. This concept is shown in Figure 3.

To change the joint's effective stiffness k_j a spring with constant k_s is translated along both links in a direction perpendicular to the spring force. This distance is given as d from the joint's centre of rotation θ. One of the benefits of this design is that it can have zero joint stiffness which occurs when $d = 0$, as the distance between where the spring connects to the both links will not change and hence the spring will not stretch. As the spring is translated along the links, corresponding to increasing d, the effective spring stiffness also increases as the distance between the links changes at a higher rate. This mechanism is possible because there is no direct coupling between the stiffness mechanism and the driving mechanism.

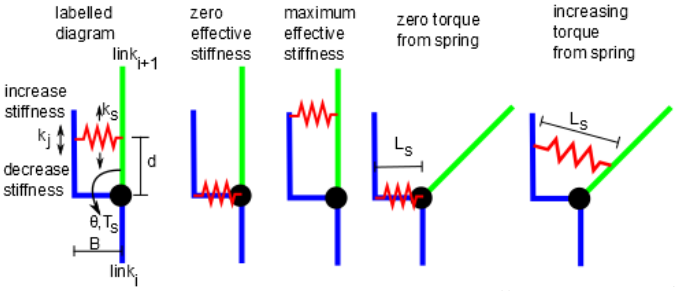

Figure 3: This diagram shows the joint's controllable stiffness mechanism in various configurations. The joint's effective stiffness is controlled by translating the spring along both links.

The total spring length, L_s is given by

$$L_s = \sqrt{2d^2(1-\cos\theta) + B^2 + 2Bd\sin\theta} \tag{24}$$

where B is the link offset distance, which is constant for a particular mechanical design, and d and θ are described above and marked in Figure 3. The spring mechanism's contribution to the joint's torque, τ_s, is given by

$$\tau_s = k_s(d^2\sin\theta + Bd\cos\theta)\left[1 - \frac{B}{L_s}\right] \tag{25}$$

Taking the derivative will give the effective spring stiffness, k_j around the joint of

$$k_j = \frac{\partial\tau_s}{\partial\theta} \tag{26}$$

$$k_j = k_s\left\{(d^2\cos\theta - Bd\sin\theta)\left[1 - \frac{B}{L_s}\right] + \frac{B(d^2\sin\theta + Bd\cos\theta)^2}{{L_s}^3}\right\} \tag{27}$$

Selection of k_s will depend on the required energy storage and range of motion. In many applications it is desirable to be able to lock the joint, such as when standing statically. In this mechanism, maximum effective stiffness is when d is at maximum and by selecting an appropriate k_s will give a high k_j and therefore the joint will be effectively rigid.

In this design the spring stiffness, k_s, is selected from two constraints: energy performance for a hop, and joint rigidity at maximum d. Given the model of the system and the flight angle to the stance angle at maximum compression the

gravitational potential energy E_g can be calculated. This potential energy is what the spring must supply, denoted E_s. Note that to simplify the equation the body mass is assumed to be greater than the link masses.

$$h_b(\varphi) = \sqrt{L_1^2 + L_2^2 - 2L_1L_2\cos\varphi} \quad (28)$$

$$E_s = E_g = Mg\left[h_j + h_b(\varphi_0) - h_b(\varphi_{max})\right] \quad (29)$$

Where φ is the angle on the inside of the leg and is derived from θ by mechanical constraints, L_1 and L_2 are the lengths of the top and bottom links respectively, h_b is the body height above the toe, and h_j is the maximum height of the toe above the ground (jump height). Then k_s can be calculated using

$$k_s = \frac{2E_s}{(L_s - B)^2} \quad (30)$$

where the value for L_s is at φ_{max}. Following on from this, the maximum spring force F_{max}, can be approximated as

$$F_{max} = k_s(L_s - B) \quad (31)$$

Due to the fact that the spring stiffness will only typically be changed during the flight phase, the duration of the flight phase (t_f) is maximum time that the stiffness should be able to be changed in

$$t_f = \sqrt{\frac{8h_j}{g}} \quad (32)$$

As discussed in the previous section the design goal is to be able to adjust the stiffness between stance phases. With this mechanism, increasing k_j during stance phase will become harder as the joint angle θ increases. However, the effective stiffness can be decreased regardless of the joint angle. Decreasing joint stiffness will allow a higher ratio of contribution from the driving actuator.

B. *Driving mechanism*

As this is a PEA design, the actuator is coupled directly between both links. Rotary actuators were rejected for two reasons. The first reason is that rotary actuators typically require large, heavy and inefficient gearboxes to increase torque output to suitable levels. These gearboxes also typically make torque control more difficult due to their high reflected inertia, necessitating the need for a spring in series with the actuator. The rotary actuators can either be mounted along the axis of rotation, or perpendicular to axis of rotation and parallel to the link. The second reason is that the mounting configuration either requires that the motor sticks out the side or the joint is wide enough to accommodate the actuator. Mounting the motors in the plane of the link requires a 90° rotation using a typically inefficient gearbox.

Linear actuators can be placed in the plane of the link without requiring a gearbox. Coupling using a single stiff wire was considered, however the energy efficiency of this transmission system is low, less than approximately 50% [9]. Instead, as shown in Figure 4, the linear actuator body is attached to the upper link using a clevis fastener and the moving shaft to a bearing on the other link. Assuming an actuator with the required force can be found, there is no need for a gearbox in this design further improving energy efficiency, decreasing joint mass, and improving control through a reduction in reflected inertia.

Given this arrangement the torque contribution from the driving actuator, τ_d is given by

$$\tau_d = \frac{A(C\sin\theta + B\cos\theta)}{\sqrt{A^2+B^2+C^2-2A(C\cos\theta - B\sin\theta)}}F_d \quad (33)$$

where A is the distance to the actuators clevis pin from joint's centre of rotation and C is the distance to the bearing that connects to the end of the shaft as shown in Figure 4.

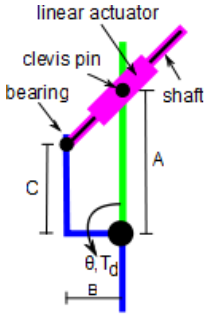

Figure 4: The linear actuator and shaft is connected between the two links using a clevis fastener and bearing. The spring is not shown.

V. Physical Implementation

This section describes the mechanical implementation of the EECSJ and its incorporation into a hopping robot. A photo of the joint and robot is shown in Figure 1. Compared to the concept diagrams the bottom link has a cantor offset of 30 degrees in the θ direction in order to allow greater range of motion before the back of the bottom link hits the ground.

Given a desired mass of $M = 0.3kg$, $L_s = 22mm$, φ_0= 150 φ_{max}= 100 degrees and using the equations given above, this gives a k_s of 2400 N/m, $F_{max} = 19.2N$ and with a desired jump height of 40mm, t_f= 0.181 s.

A. *Stiffness mechanism*

Each end of the spring was attached to a runner for translation along a rotating lead-screw, which was driven by a rotary DC motor. A lead-screw mechanism resists undesirable changes to the set runner position and is self-locking. A Faulhaber EN1524SR-012 was subsequently chosen to drive each side of the stiffness mechanism.

In this paper the focus is on demonstrating the conceptual design, rather than an optimal mechanical implementation. It is possible to implement this stiffness mechanism with only a single actuator and a coupling linkage, however, the mechanical design was simpler using two actuators. Ignoring the added mass, using a single actuator instead of two actuators will not save energy to move the spring. In fact, the typically significant losses in a coupling linkage could offset any benefits.

Position feedback of the spring runner is provided by a magnetic membrane potentiometer and a magnet mounted in the runner. As the runner translates along the lead-screw, the magnet engages a wiper in the potentiometer, encoding the absolute position of the runner.

B. *Driving actuator*

A range of linear actuators were considered for this design including solenoids, voice coils, piezoelectric and three-phase DC coils. Piezoelectric actuators were rejected because their peak force is too low for medium to large legged robots and have low shaft speeds. Voice coils were considered over solenoids due to their more linear force versus stroke characteristic and that generally voice coils can be operated in both directions without a return spring.

The new range of Faulhaber Quickshaft 3-phase linear actuators have a high peak power to mass and peak power to volume ratio. Under force control, they are also back drivable. The Quickshaft actuators have integrated Hall Effect sensors for position feedback. This implementation uses the LM 1247-020-01.

C. *Hopping Knee Joint*

In order to demonstrate that the effectiveness of the parallel configuration and performance of the EECSJ it is implemented as the knee joint of a hopping robot. The ends of the joint's links are constrained to move the vertical direction by bearings on a linear rail. The foot is unable to rotate. The foot height and mass height are measured using encoders. The foot height is measured using a linear encoder attached to the foot and the linear rail. The joint angle is derived from the extension of the linear actuator as given by the inbuilt Hall Effect sensors. The mass height is derived using the joint angle and foot height. The total mass of the leg, including the foot and runners is 0.275kg. Adding 0.365kg of body mass increased the total mass to 0.64kg.

D. *Hopping Controller*

The goal of the controller is to hop with the EECSJ's natural periodic motion. A positive feedback controller was implemented using only internal state information, in this case the actuator's direction of movement. For continuous operation, the actuator will apply a force equivalent to the rated maximum continuous current draw in the direction of motion of the leg giving a continuous hop motion. The most significant amount of energy loss during the jump cycle is during the stance phase; as such, the actuator only needs to supply energy during the stance phase to maintain hopping. This part of the controller provides increased energy efficiency, as the actuator isn't providing wasted energy during the flight phase. Based on this strategy, the jump height of the EECSJ would approach a steady state condition where the amount of energy lost to damping and restitution during stance would be identical to the amount of energy put into the system using the actuator.

The other source of energy loss is the jump cycle is due to restitution at toe-down. Initial experiments indicated that during normal operation of this controller there would be a short "bounce" of the toe after the first contact, causing additional restitution losses. A small pretensioning force was applied to the spring by the actuator during flight, the consequence of which is that the normalizing force holding the toe in contact with the ground is increased during the initial contact, significantly reducing the bounce magnitude.

VI. Study: Continuous and Peak Jumping

This study demonstrates the EECSJ's hopping performance while the stiffness mechanism position is maintained (constant d). The leg is able to continuously hop to a height of 6mm. This study investigated the continuous and maximum jump height that could be achieved using the EECSJ by working at the actuators continuous rated current (0.55 amps) then briefly working at the actuator's rated peak current (1.66 Amps). After several stable steady state hops, the force applied by the actuator for the control strategy was increased to be the equivalent of the maximum current rating for the actuator This increase in energy output from the actuator results in a higher jump, albeit one that cannot be sustained for long to avoid overheating the actuator. Figure 5 shows the toe height which shows a continuous jump height of 6mm and peak height of 14mm. The centre of mass has a delta height of 50mm. Figure 6 has an image sequence that shows the maximum jump.

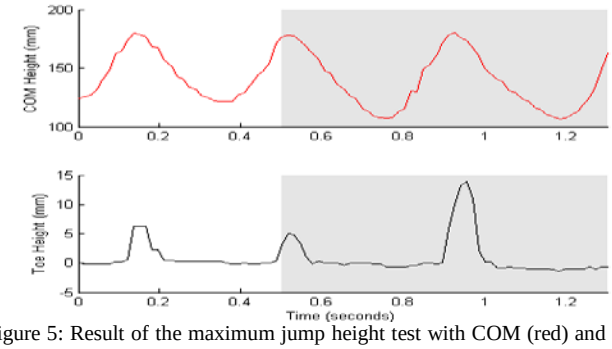

Figure 5: Result of the maximum jump height test with COM (red) and toe height (black). At 0.5 seconds the controller is changed from applying maximum continuous force to applying peak force (approximately 3 times larger), resulting in a higher jump at ~0.95 seconds of 14 mm. The fact that the increased height doesn't significantly carry forward into the COM height is attributed to significant losses in restitution at the moment of toe-up and in damping from the linear rail that constrains the motion of the leg.

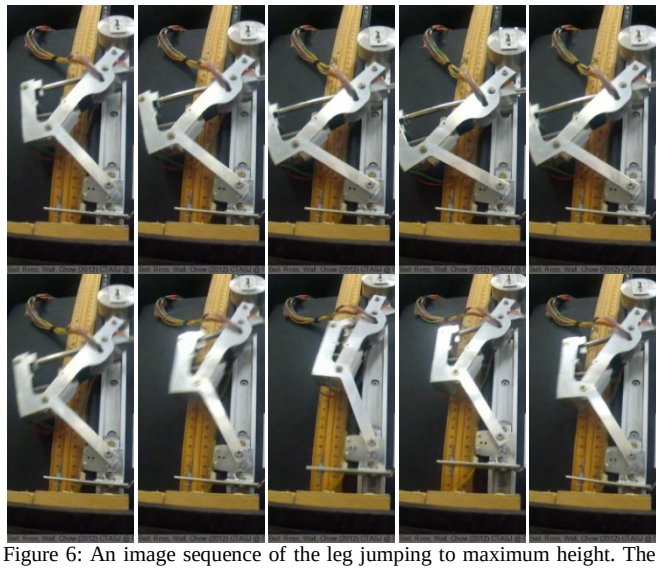

Figure 6: An image sequence of the leg jumping to maximum height. The images start at 1 and run from left to right, top to bottom. The time between images is ~42ms. In image 4 the leg is at maximum bend, in image 7 the foot is jump about to lift off, and in image 9 the foot is at its peak height. See the attached video for a demonstration of continuous and peak jumping.

VII. Study: Controlling Hopping Frequency

This study explores the performance of the controllable stiffness mechanism in controlling hopping frequency. The study begins by exploring the basic capabilities of the joint, including results demonstrating that stiffness can be changed during flight phase. Then the study has results showing that hopping frequency and stance duration can be controlled via joint stiffness.

The limit to the joint's range of motion is the plastic deformation of the springs. At 100% of the lead screw, equivalent to maximum stiffness the joint's range of motion during motion is 45 degrees; at 70% the range of motion is 70 degrees. The joint's range of motion, particularly at high stiffness, is small compared to other VSAs however is comparable to a knee's normal operating range. The deflection at maximum stiffness when static is 2.5^{o} supporting the 0.365kg mass which is considered highly rigid. The joint would be more rigid with stronger springs.

A. *Stiffness change time*

A PD controller sets the position of the stiffness mechanism, given by feedback from the linear magnetic sensors. The result of changing the stiffness in the unloaded case is shown in Figure 7 and shows that the mechanism was able to change the stiffness from maximum to minimum in 0.2 seconds lagging the ideal desired position. The calculated duration of the average flight phase was 0.1 seconds, meaning that the stiffness could not be completely changed during a single flight. In effect, this should not be a problem. With the given mass and spring value, the leg is unable to jump at stiffness lead screw positions lower than 70%, so the mechanism is capable of changing the stiffness from the maximum to a position where there is no stable hopping during a single flight phase. At positions lower than 70%, the leg collapsed. Changing stiffness during a flight phase is shown in Figure 8 with the consequential change in toe height performance for the next jump.

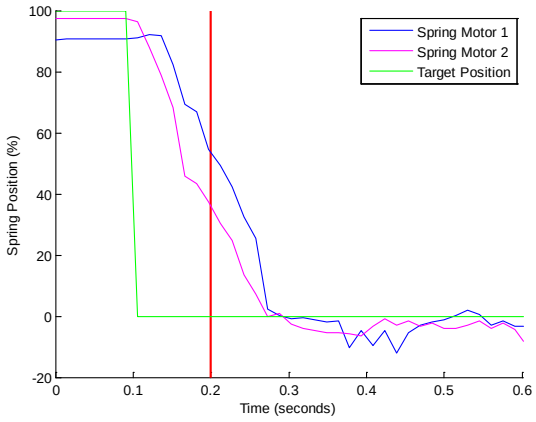

Figure 7: This figure shows the response of the spring mechanism, which correlates with the joint stiffness, to a large step change in desired position. The red line (vertical line at 0.2 seconds) indicates the time at which the leg would land on the ground (under normal hopping operation), were it to be used in this fashion. Therefore the joint's stiffness could not be changed from 100% to 0% in one step, however this is unlikely to be a major problem.

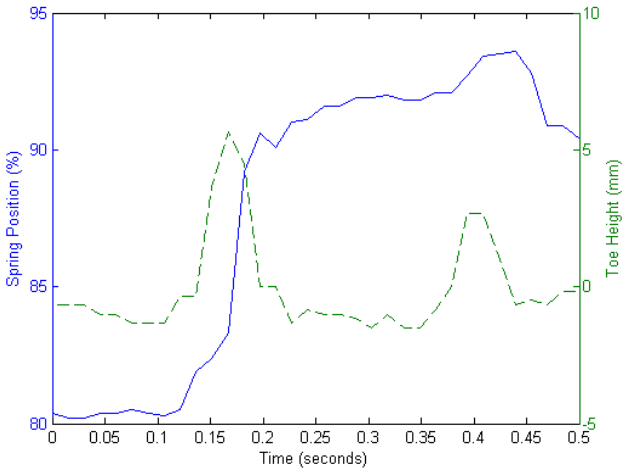

Figure 8: The position of the spring motor being changed during the flight phase of the leg. In this case the stiffness is shown to be reliably changed from 80 to 90% in a single jump.

B. *Results of changing stiffness on EECSJ*

Figure 9 demonstrates the change in hopping characteristics as the stiffness of the joint is controlled. It shows that the jump frequency is controllable between 2.2 Hz and 4.6 Hz. Note that hopping frequency and stance duration are not directly related, although there is a high correlation.

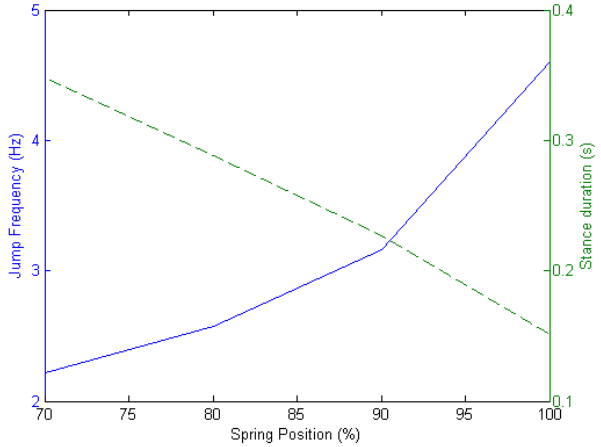

Figure 9: Jump frequency and stance duration changes as a result of changing the spring position. Approximately, the stiffness changes from 2.2 Hz to 4.6 Hz and the duration from 0.35 to 0.15s for this particular mass and spring strength. A limited range of spring positions were investigated due to the fact that at lower positions the effective leg stiffness was insufficient to allow hopping for the body mass.

VIII. Discussion

The analytical derivation in Section 3 demonstrates that the PEA configuration is more energy efficient than the SEA for SLIP motion. This result is validated by results from our physical implementation. The leg hops with a relatively low power actuator and hence demonstrates the effectiveness of the parallel arrangement in reducing the energy cost, making it possible to hop at all. It is important to note that a hybrid joint that also has a spring in series with the actuator may provide other previously reported benefits to hopping such as higher bandwidth compliance. However, this paper has reported on the benefits of the parallel arrangement of the

elastic elements.

The results show only a small hopping height, due to the linear rail and bearings providing relatively significant damping, and the high relative mass of the aluminium in the leg. The simple positive feedback controller was possible as the Faulhaber LM series primary driving actuator in this configuration did not require a gearbox, allowing torque control without a series spring. The typical 280% improvement in jump height from continuous to peak operation correlates well with the three times increase in energy supplied by the actuator. This peak operation will be needed to handle special jump cases or external disturbance to bring the joint back into normal operation.

The controllable stiffness results demonstrate that the mechanism works as designed, allowing the hopping frequency and stance duration to more than double across approximately 30% of the stiffness position range. As the robot's gait characteristics can be controlled by changing the joint's stiffness, the primary actuator does not require energy to compete against a natural motion of the fixed spring. This gait change will allow the robot for example to change hopping frequency without requiring the primary actuator to add more energy to the system. The gait change will also help with trajectory control in the face of changes in robot mass, external disturbances, or changing ground hardness.

As far as the authors are aware this is the first published use of Faulhaber LM series actuators in a robotics application. They have proven to be an excellent actuator with high force output compared to other actuators.

Table 1 has a summary of the results and specifications for the EECSJ.

Table 1. Summary of the EECSJ results. Note that the range of motion is dependent on a maximum L_s which is when the spring will deform plastically.

Specification	Value
Actual k_s (combined)	2040N/m
Range of motion (shaft stroke)	0 – 82 deg
Range of motion (spring deformation at 100% stiffness)	0 – 45 deg
Range of motion (spring deformation at 70% stiffness)	0 – 70 deg
Range of effective stiffness	0 – 1.275 Nm
Deflection at maximum stiffness	2.5 deg
Range of jump frequencies (70-100% position)	2.2Hz to 4.6Hz
Range of stance duration (70 – 100% position)	0.35s – 0.15s
Mass (joint and links only)	0.446kg
Continuous jump height (toe, COM in mm)	5mm, 14mm
Peak jump height (toe, COM in mm)	14mm, 14mm

It is possible to have a simpler stiffness mechanism concept, by permanently fixing the distal end of the spring (the left side in Figure 3), only allowing the other side to translate. The compromise is that if the spring is fixed at one end then theoretically the range of motion is limited to less than 90^o, compared with translating the spring along both links which allows up to nearly 180^o. In our particular mechanical implementation this was irrelevant as the shaft stroke of the driving actuator limited the range of motion to 82^o. However, the full range of many animal and robot joints is over 90^o, therefore it is possible that future implementations will require the extra range.

IX. Conclusion

The current generation of legged robots are either tethered or have short run times due to inefficient configuration of joint mechanisms. This paper analytically demonstrated that a parallel configuration of the elastic and actuator elements is more energy efficient than the typical series configuration. The conceptual design and implementation addresses the caveat of a parallel configuration with a controllable joint stiffness mechanism that allows control of hopping frequency and stance duration. As joint stiffness is controllable, relatively powerful springs can be used for increased energy storage and release. Hence, this will allow gait control for energy efficient legged locomotion.

ACKNOWLEDGEMENT

This work was supported in part by the Australian Research Council and National Health and Medical Research Council Special Research Initiative TS0669699, "Thinking Systems: Navigating through Real and Conceptual Spaces" and the New Staff Research Start-Up Fund RM2011000971 "A novel elastic joint for the next generation of legged locomotion" at The University of Queensland, Australia.

References

[1] T. A. McMahon and G. C. Cheng, "The mechanics of running: How does stiffness couple with speed? ," *Journal of Biomechanics*, vol. 23, 1990.

[2] D. P. Ferris, K. Liang, and C. T. Farley, "Runners adjust leg stiffness for their first step on a new running surface " *Journal of Biomechanics*, vol. 32, 1999.

[3] G. A. Pratt and M. M. Williamson, "Series elastic actuators," in *International Conference on Intelligent Robots and Systems*, 1995.

[4] J. W. Hurst, J. E. Chestnutt, and A. A. Rizzi, "The Actuator With Mechanically Adjustable Series Compliance," *IEEE Transactions on Robotics*, vol. 26, 2010.

[5] A. Jafari, N. G. Tsagarakis, B. Vanderborght, and D. G. Caldwell, "A Novel Actuator with Adjustable Stiffness (AwAS)," in *International Conference on Intelligent Robots and Systems (IROS2010)*, Taipei, Taiwan, 2010.

[6] A. Jafari, N. G. Tsagarakis, and D. G. Caldwell, "AwAS-II: A new Actuator with Adjustable Stiffness based on the novel principle of adaptable pivot point and variable lever ratio," presented at the IEEE International Conference on Robotics and Automation, Shanghai, China, 2011.

[7] B. Vanderborght, N. G. Tsagarakis, R. V. Ham, I. Thorson, and D. G. Caldwell, "MACCEPA 2.0: compliant actuator used for energy efficient hopping robot Chobino1D " *Autonomous Robots*, vol. 31, pp. 55-65, 2011.

[8] S. Wolf and G. Hirzinger, "A New Variable Stiffness Design: Matching Requirements of the Next Robot Generation," presented at the 2008 IEEE International Conference on Robotics and Automation, Pasadena, USA, 2008.

[9] S. Rutishauser, "Cheetah - compliant quadruped robot," Swiss Federal Institute of Technology, Lausanne2008.